

# Semi-Lagrangian simulations on polar grids: from diocotron instability to ITG turbulence



Crouseilles<sup>1</sup> Glanc<sup>2</sup> Hirstoaga<sup>2</sup> Madaule<sup>3</sup> Mehrenberger<sup>2,4</sup> Pétri<sup>5</sup>

<sup>1</sup> INRIA-Rennes & IRMAR, Rennes, France, <sup>2</sup> INRIA-Nancy & IRMA, Strasbourg, France <sup>3</sup> Institut Jean Lamour, Nancy, France, <sup>4</sup> Max-Planck-Institut für Plasmaphysik, Garching, Germany <sup>5</sup> Observatoire Astronomique de Strasbourg, Strasbourg, France

nicolas.crouseilles@inria.fr, glanc@math.unistra.fr,  
hirstoaga@math.unistra.fr, madaule.eric@orange.fr,  
mehrenbe@math.unistra.fr, jerome.petri@astro.unistra.fr

## Abstract

While developing a new semi-Lagrangian solver, the gap between a linear Landau run in  $1D \times 1D$  and a  $5D$  gyrokinetic simulation in toroidal geometry is quite huge. Intermediate test cases are welcome for checking the code. We consider here as building block, a  $2D$  guiding center type equation on an annulus:

$$\partial_t f - \frac{\partial_\theta \Phi}{r} \partial_r f + \frac{\partial_r \Phi}{r} \partial_\theta f = 0, \quad t \in [0, T], \quad (1)$$

with  $(r, \theta) \in \Omega = [r_{\min}, r_{\max}] \times [0, 2\pi]$ , where the potential  $\Phi$  solves a Poisson type equation. We first revisit a  $2D$  test case previously done with a PIC approach [6] and detail the boundary conditions. We then consider a  $4D$  drift kinetic slab simulation [2] for which we give some first results of a new conservative method.

## 1. Diocotron instability test case [3]

We consider  $\rho = f$ , solution of (1), with  $\Phi$  solving Poisson equation:

$$-\partial_r^2 \Phi - \frac{1}{r} \partial_r \Phi - \frac{1}{r^2} \partial_\theta^2 \Phi = \gamma \rho,$$

where  $\gamma \in \{-1, 1\}$ , depending on the context (astro/plasma physics). We define the electric energy

$$\mathcal{E}(t) = \int_{\Omega} r |\partial_r \Phi|^2 + \frac{1}{r} |\partial_\theta \Phi|^2 dr d\theta, \quad (2)$$

and the mass

$$\mathcal{M}(t) = \int_{\Omega} r \rho dr d\theta. \quad (3)$$

We take Dirichlet boundary condition at  $r_{\max}$ :

$$\Phi(r_{\max}) = 0$$

At  $r_{\min}$ , we take either Dirichlet boundary condition or the following condition, named **Neumann mode 0** which differ from Neumann boundary condition (the latter being  $\partial_r \Phi(r, r_{\min}, \theta) = 0$ ):

• Neumann boundary condition at  $r_{\min}$  for the Fourier mode 0 in  $\theta$ :

$$\int_0^{2\pi} \partial_r \Phi(t, r_{\min}, \theta) d\theta = 0,$$

• Dirichlet boundary condition at  $r_{\min}$  for the other modes, which reads

$$\Phi(t, r_{\min}, \theta) = \frac{1}{2\pi} \int_0^{2\pi} \Phi(t, r_{\min}, \theta') d\theta'$$

We then have the following result:

- For such boundary conditions, mass and energy are constant in time
- If we move to Neumann boundary condition at  $r_{\min}$ , this may not remain true.

We consider the following initial data [Davidson, 1990]

$$\rho(0, r, \theta) = \begin{cases} 0, & r_{\min} \leq r < r^-, \\ 1 + \epsilon \cos(\ell\theta), & r^- \leq r \leq r^+, \\ 0, & r^+ < r \leq r_{\max}, \end{cases}$$

where  $\epsilon$  is a small parameter.

Linearized problem leads then here to explicit solutions

$$\rho(t, r, \theta) \simeq n_0(r) + \epsilon \hat{n}_{1,\ell}(r) \exp(i\ell\theta) \exp(-i\omega t/\gamma) + O(\epsilon^2)$$

$$\Phi(t, r, \theta) \simeq \gamma \hat{\Phi}_0(r) + \epsilon \gamma \hat{\Phi}_{1,\ell}(r) \exp(i\ell\theta) \exp(-i\omega t/\gamma) + O(\epsilon^2)$$

Analytical growth rates  $|\Im(\omega)|$  of the linear phase are obtained for all the discussed boundary conditions and comparison is made with BSL method on  $128 \times 128$  grid,  $\Delta t = 0.05$ ,  $r_{\min} = 1$ ,  $r_{\max} = 10$ ,  $\gamma = 1$ .

$\ell$	$r^-$	$r^+$	$\Im(\omega)$	analytical
2	4	5	0.2875, $t \in [26, 55]$	0.288739227554270
3	4	5	0.3667, $t \in [26, 72]$	0.367315895142460
4	4	5	0.3852, $t \in [26, 51]$	0.384081542249742
7	6	7	0.3424, $t \in [26, 61]$	0.337573424025866

Table 1: Dirichlet boundary condition

$\ell$	$r^-$	$r^+$	$\Im(\omega)$	analytical
2	4	5	0.0719, $t \in [93, 138]$	0.0717643545314240
3	4	5	0.2264, $t \in [33, 87]$	0.226724091815516
4	4	5	0.2991, $t \in [34, 69]$	0.298891133128847
7	6	7	0.3338, $t \in [35, 53]$	0.330764942142169

Table 2: Neumann mode 0 boundary condition

$\ell$	$r^-$	$r^+$	$\Im(\omega)$	analytical
2	4	5	0.0672, $t \in [89, 151]$	0.067338570606553
3	4	5	0.2263, $t \in [32, 89]$	0.226665019518819
4	4	5	0.2991, $t \in [34, 69]$	0.298891598934172
7	6	7	0.3338, $t \in [35, 53]$	0.330764942148054

Table 3: Neumann boundary condition

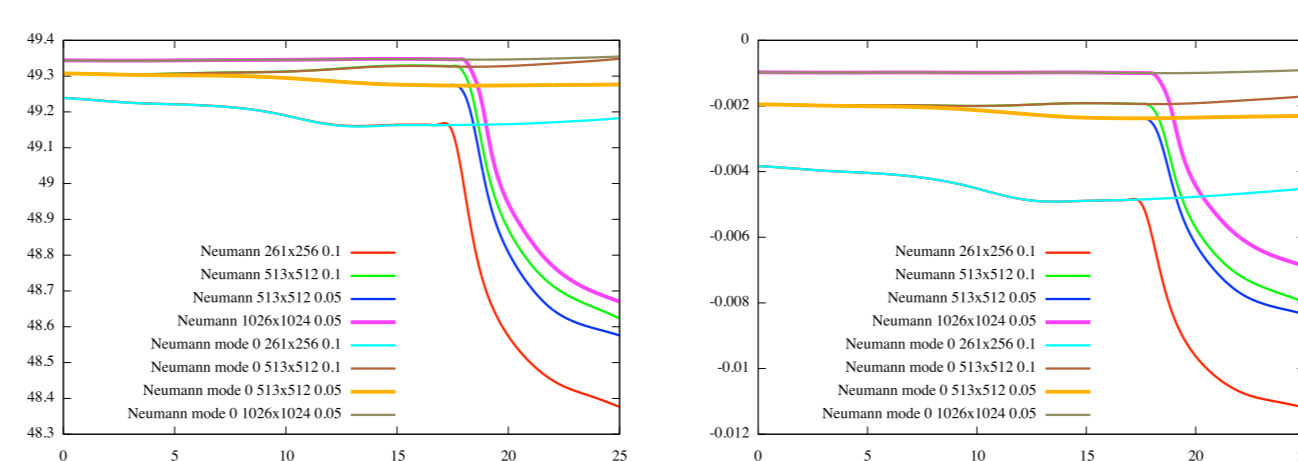


Figure 1: Evolution of  $\mathcal{E}(t)$  (left) and  $\mathcal{M}(t)$  (right) for different grid sizes and  $\Delta t$

## 2. 4D slab drift kinetic Vlasov equation

We look for  $f = f(t, r, \theta, z, v)$  [2], satisfying

$$\partial_t f - \frac{\partial_\theta \Phi}{r} \partial_r f + \frac{\partial_r \Phi}{r} \partial_\theta f + v \partial_z f - \partial_z \phi \partial_v f = 0, \quad (4)$$

for  $(r, \theta, z, v) \in \Omega \times [0, L] \times [-v_{\max}, v_{\max}]$ .

Potential  $\phi = \phi(r, \theta, z)$  solves the quasi neutral equation

$$-\left(\partial_r^2 \phi + \left(\frac{1}{r} + \frac{\partial_r n_0(r)}{n_0(r)}\right) \partial_r \phi + \frac{1}{r^2} \partial_\theta^2 \phi\right) + \frac{1}{T_e(r)} (\phi - \langle \phi \rangle) = \frac{1}{n_0(r)} \int f dv - 1, \quad \langle \phi \rangle = \frac{1}{L} \int_0^L \phi(r, \theta, z) dz.$$

The initial function is

$$f(0, r, \theta, z, v) = f_{\text{eq}}(r, v) (1 + \epsilon \exp(-\frac{(r-r_p)^2}{\delta r}) \cos(\frac{2\pi n}{L} z + m\theta)),$$

with equilibrium function

$$f_{\text{eq}}(r, v) = \frac{n_0(r) \exp(-\frac{v^2}{2T_i(r)})}{(2\pi T_i(r))^{1/2}}.$$

The profiles have here analytical expressions

$$\mathcal{P}(r) = C_{\mathcal{P}} \exp(-\kappa_{\mathcal{P}} \delta r \tanh(\frac{r-r_p}{\delta r})), \quad \mathcal{P} \in \{T_i, T_e, n_0\}$$

$$C_{T_i} = C_{T_e} = 1, \quad C_{n_0} = \frac{r_{\max} - r_{\min}}{\int_{r_{\min}}^{r_{\max}} \exp(-\kappa_{n_0} \delta r \tanh(\frac{r-r_p}{\delta r})) dr}$$

We consider the parameters of [1] (MEDIUM case)

$$r_{\min} = 0.1, \quad r_{\max} = 14.5, \quad \kappa_{n_0} = 0.055, \quad \kappa_{T_i} = \kappa_{T_e} = 0.27586,$$

$$\delta r_{T_i} = \delta r_{T_e} = \frac{\delta r_{n_0}}{2} = 1.45, \quad \epsilon = 10^{-6}, \quad n = 1, \quad m = 5,$$

$$L = 1506.759067, \quad r_p = \frac{r_{\min} + r_{\max}}{2}, \quad \delta r = \frac{4\delta r_{n_0}}{\delta r_{T_i}}.$$

Analytical growth rates are no more available, but we can check the linear phase with recent results [1], p19.

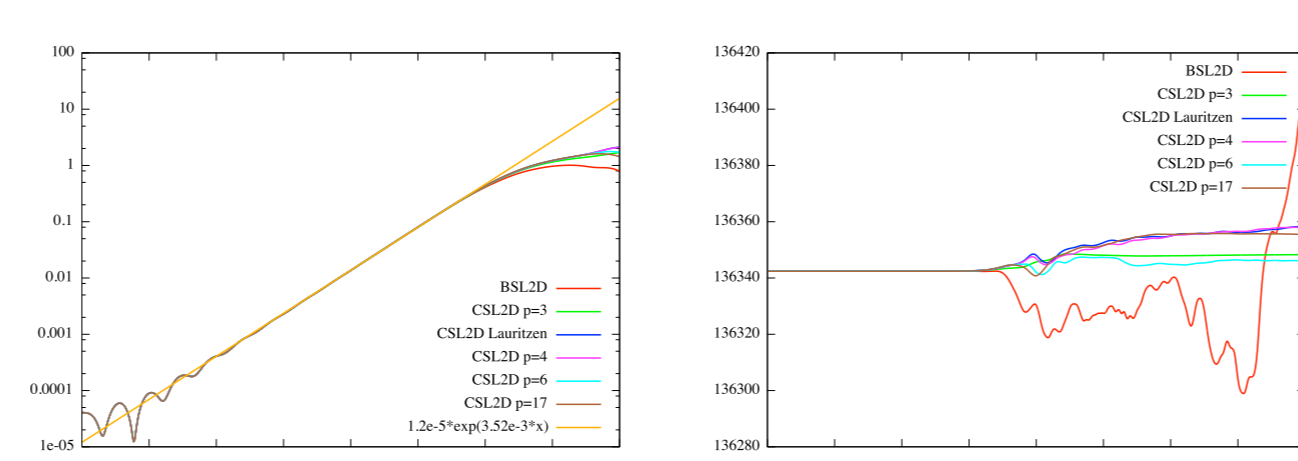


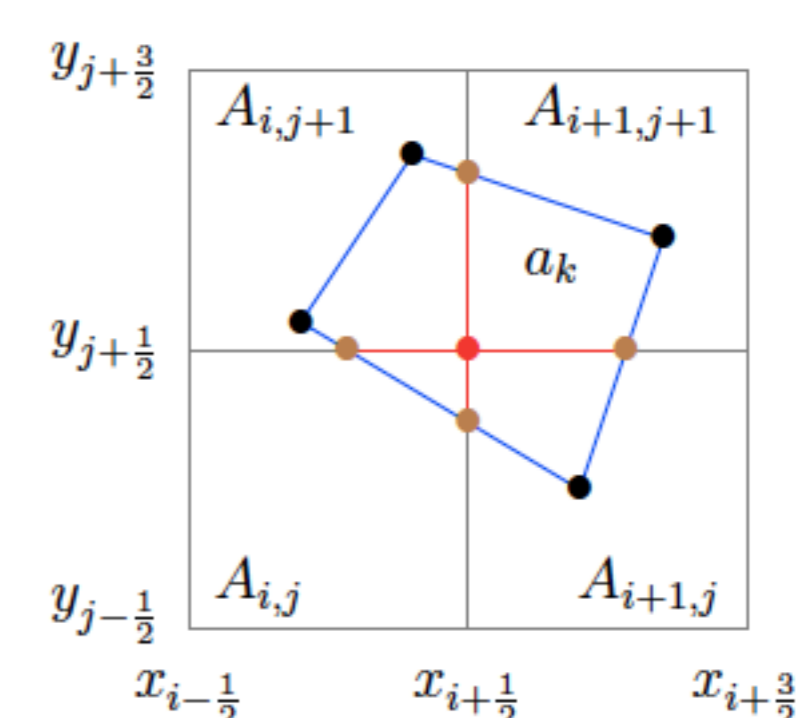
Figure 2: Evolution of  $\int \int \Phi^2(r_p, \theta, z) d\theta dz$  (left), mass (right) on  $32 \times 32 \times 32 \times 64$  grid, with  $\Delta t = 8$ ,  $v_{\max} = 7.32$

## 3. Description of the classical method

As in [2], the BSL method is used. The following options are here:

- constant advection in  $z, v$ , with cubic splines (periodic)
- $2D$  advection in  $(r, \theta)$  with cubic splines
  - Verlet algorithm for the characteristics
  - linear interpolation of the fields
- splitting and predictor corrector for time loop
- fields derivatives with cubic splines in  $r, \theta$  and second order finite differences in  $z$
- Poisson/quasi neutral with FFT in  $\theta$  and second order finite difference in  $r$ .

## 4. A new 2D conservative method, following [5]



- unknowns are cell values  $\bar{f}_{i,j}^n$
- backward displacement of cell
- order  $p$  compact reconstruction of edge values  $\bar{f}_{i,j\pm}^n$ ,  $\bar{f}_{i\pm,j}^n$  and point values  $\bar{f}_{i\pm,j\pm}^n$
- polynomial on  $A_{i,j}$ :  $\sum_{\alpha,\beta \leq 2} c_{\alpha,\beta} x^\alpha y^\beta$
- contribution of  $x^\alpha y^\beta$  on each edge of  $a_k \cap A_{i,j}$  with Stokes formula

Adaptations w.r.t. uniform periodic case are needed as in [4] for the FSL method.

- multiply by jacobian, since conservative form is on  $g(t, r, \theta) = r f(t, r, \theta)$ , satisfying

$$\partial_t g - \partial_r \left( \frac{\partial_\theta \Phi}{r} g \right) + \partial_\theta \left( \frac{\partial_r \Phi}{r} g \right) = 0$$

- work on  $f - f_{\text{eq}}$  for non zero boundary conditions (also used for BSL)

## 5. Conclusion/ future work

- description of  $2D$  and  $4D$  test cases on polar geometry for semi-Lagrangian solvers
- development of a new conservative method
- ongoing implementation in a dedicated library [7]

## References

- [1] Coulette, Besse, JCP 248 (2013)
- [2] Grandgirard et al., JCP 217 (2006)
- [3] Madaule et al., hal-00841504
- [4] Latu et al., INRIA Research Report 8054
- [5] Lauritzen et al, JCP 229 (2010)
- [6] Petri, Astronomy & Astrophysics, May 2009
- [7] SELALIB, <http://selalib.gforge.inria.fr/>